文章编号：1001-9014(XXXX)XX-0001-11

DOI:10.11972/j.issn.1001-9014.XXXX.XX.001

Moving mirror speed compound control of the Fourier transform spectrometer based on T-method

HUANG Ying[1,2,3], DUAN Juan[1,2*], GUO Qian[1,2], DING Lei[1,2*], HUA Jian-Wen[1,2]

(1. Shanghai Institutes of Technical Physics, Chinese Academy of Sciences, Shanghai 200083, China;
2. State Key Laboratory of Infrared Physics, Chinese Academy of Sciences, Shanghai 200083, China;
3. University of Chinese Academy of Sciences, Beijing 100049, China)

Abstract: The Fourier transform spectrometer (FTS) is a precision infrared detection instrument. It adopts Michelson interference splitting, and the moving mirror is one of the core components. The uniformity and stability of the moving mirror's speed directly affect the quality of the subsequent interferogram, so it is necessary to carry out high-precision motion control of the moving mirror. For some FTS with moving mirror in low-speed motion, the traditional M-method can no longer meet the requirements of speed measurement accuracy. In addition, when the moving mirror moves at a low speed, the speed stability is more easily affected by external mechanical disturbance. Based on the stability requirement of the low-speed moving mirror, this paper studies the motion control of the moving mirror based on the T-method measuring speed. It proposes a high-precision algorithm to obtain the measured and expected value of the velocity. By establishing the mathematical model and dynamic equation of the controlled object, the speed feedforward input is obtained, and then the compound speed controller based on the feedforward control is designed. The control algorithm is implemented by the FPGA hardware platform and applied to the FTS. The experimental results show that the peak-to-peak velocity error is 0.0182, and the root mean square (RMS) velocity error is 0.0027. To test the anti-interference ability of the moving mirror speed control system, the sinusoidal excitation force of 5 mg, 7.5 mg, and 10 mg is applied in the moving mirror motion direction on the FTS platform. Under each given magnitude, the scanning of each frequency point in 2~200 Hz is carried out. The experimental results show that the peak-peak velocity error and the RMS velocity error are proportional to the excitation magnitude. Under the 10 mg excitation, the maximum peak-to-peak velocity error is 0.1405, and the maximum RMS velocity error is 0.0448. After analysis, the speed stability of the moving mirror can still meet the performance requirements of the FTS. This design provides a technical means for realizing the speed control of the moving mirror with low speed and high stability. Also, it makes the FTS have wider applications.

Key words: Fourier transform spectrometer, speed control, T-method, speed feedforward, velocity uniformity

基于T法的光谱仪动镜速度复合控制

黄 莹[1,2,3], 段 娟[1,2*], 郭 倩[1,2], 丁 雷[1,2*], 华建文[1,2]

(1. 中国科学院上海技术物理研究所,上海 200083;
2. 红外科学与技术全国重点实验室,上海 200083;
3. 中国科学院大学,北京 100049)

摘要:傅里叶变换光谱仪是一种精密的红外探测仪器,它采用迈克尔逊式干涉分光方式,动镜是其中一个核心部件。动镜运动速度的均匀性和稳定性直接影响了后续干涉图的质量,所以必须对动镜进行高精度的运动控制。对于某些动镜低速应用场合的傅里叶光谱仪,常规的M法测速已经不能满足测速精度的要求了。另外,动镜低速运动时,速度稳定性更容易受外界力学扰动的影响。基于动镜低速运动的平稳性需求,文中

Received date: 2025-01-16, **revised date**: 2025-02-24 **收稿日期**:2025-01-16,**修回日期**:2025-02-24

Foundation items: Supported by the National Key Research and Development Program of China (2023YFB3905400)

Biography: HUANG Ying (1995-), female, Fuzhou, Ph. D. Research area involves motion control of the Fourier transform spectrometer. E-mail: 690803501@qq.com.

* **Corresponding authors**: E-mail: duanjuan@mail.sitp.ac.cn; leiding@mail.sitp.ac.cn

对基于T法测速的动镜运动控制技术进行了研究,提出了求取速度实测值和速度期望值的高精度算法,并通过建立被控对象的数学模型和动力学方程,得到速度前馈控制量,进而设计了基于速度前馈的复合速度控制器。该设计的动镜速度控制算法由FPGA硬件平台实现,并应用于傅里叶光谱仪实验平台。实验结果表明,采用T法测速控制系统获得动镜运动匀速区速度峰峰值误差是0.0182,速度均方根值误差是0.0027。为测试文中动镜速度控制系统的抗干扰能力,在干涉仪安装平台动镜运动方向分别施加5 mg、7.5 mg、10 mg的正弦激励力,在每个给定量级的激励力下,进行了2~200 Hz频率范围内各频率点的扫描,实验结果表明,速度误差峰峰值和速度误差均方根值和正弦激励的幅值基本成正比例关系。在10 mg时各频率点的力学激励下,速度误差峰峰值最大是0.1405,速度误差均方根值最大是0.0448,经分析动镜速度平稳性依然能满足傅里叶光谱仪的性能要求。该设计为傅里叶光谱仪低速高平稳性动镜速度控制的实现提供了一种技术途径,同时也使得傅里叶光谱仪有了更广阔的应用场景。

关 键 词:傅里叶光谱仪;速度控制;T法测速;速度前馈;速度均匀性

中图分类号:TP731 **文献标识码**:A

Introduction

The Fourier transform spectrometer (FTS) is an infrared detection instrument. It collects the interference signal of the target's infrared radiation and obtains the infrared spectrum information through the Fourier transform. The FTS is widely used in atmospheric detection, chemical analysis, sample detection, and so on[1-6]. It adopts the classical Michelson interference splitting, and the moving mirror is a core component. To obtain good interferogram quality through equal optical path difference sampling of the interference signal, the moving mirror must move back and forth at a uniform speed. The velocity uniformity in the uniform region is an important performance index affecting the spectral quality, so it is necessary to design a controller to control the moving mirror speed precisely.

The moving mirror system of the FTS usually has a reference laser interference system. The traditional speed measurement method is to count the reference laser interference pulses, measuring the moving mirror displacement in a period to obtain the current speed of the moving mirror, that is M-method[7]. A moving mirror control system for spaceborne FTS is described in the literature[8]. Its motion system consists of elastic supports, flat mirrors, and a voice coil motor. The control system adopts single position-loop control to achieve control of the position and speed of the moving mirror. The speed measuring method is the M-method. The final control effect is that the error of the peak-to-peak velocity in the uniform region is 0.088, and the error of the RMS velocity is 0.014. The Atmospheric Chemistry Experiment (ACE) is the mission selected by the Canadian Space Agency for its next science satellite, SCISAT-1. The infrared FTS is the primary element. In the control system, the servo motor provides position control of the rotary arm in a closed-loop configuration using the M-method. The position profile is generated by an FPGA. A Proportional-Integrator-Derivative-Filter (PIDF) servo compensation is implemented and coupled with a feedforward controller[9]. M-method is relatively simple to implement, but its disadvantage is that the measurement accuracy is low, especially in the low-speed moving mirror control system, its measurement accuracy will be difficult to meet the performance requirements. Thermal Emission Spectrometer (Mini-TES) is a single-pixel FTS used to measure thermal emission for mapping surface minerals on Mars. The control system of the moving mirror is a speed feedback controller, which uses a voice coil motor. The servo is a digital servo that counts the time between a fringe signal's zero crossings to generate a velocity error signal. The analog portion of the servo uses the tachometer signal from the motor to assist in headback compensation[10]. Thereby, there is no moving mirror speed control system based on combining the T-method[11] speed measurement and speed feedforward. This paper makes an exploratory study on the control system combining T-method and feedforward.

T-method is to obtain the current speed of the moving mirror by measuring the time it takes to move a certain distance. Then compare the time with the expected time to acquire the speed error. Since the frequency of the time counting clock is only limited to the local clock, the counting value is much higher than that of the M-method, which greatly improves the measurement accuracy. In addition, introducing feedforward control in the control system can improve the response performance of the moving mirror to the desired command. By establishing the mathematical model of the moving mirror system and the expected motion law, we obtain the precise feedforward inputs based on the controlled object. Finally, we use the FPGA development platform to realize the composite speed control algorithm based on T-method speed measurement, speed feedforward, and speed-loop controller, carrying out the performance verification experiment on the FTS. The experimental results show that without vibration, the peak-to-peak velocity error in the uniform region is 0.0182, and the RMS velocity error is 0.0027. Apply 5mg, 7.5mg, and 10mg sine excitation force in the moving mirror motion direction for frequency-fixed scanning. The fixed frequency step is 2Hz in 2-120Hz and 5Hz in 120-200Hz. Under the 5mg, 7.5mg, and 10mg vibration, the maximum peak-to-peak velocity error is 0.0724, 0.1087, and 0.1405 respectively, and the maximum RMS velocity error is 0.0225, 0.0334, and 0.0448. Taking the velocity error of 0.1405 as the FTS spectral inversion's input, the simulation results show that the spectrum stability caused by the velocity er-

ror is 0. 14ppm, less than 2ppm, which meets the spectrum stability requirement of the FTS. The results show the superiority of the whole control scheme, making the FTS have wider applications.

1 Moving mirror speed control system

As shown in Figure 1, the moving mirror speed control system in this paper mainly consists of a speed feedforward controller, speed expectation, speed-loop controller, speed measuring device, motion actuator, and moving mirror driving mechanism.

The driving mechanism consists of elastic translational support and a linear motor. The elastic translational support mechanism is widely used in the moving mirror system of the FTS[12-13]. It makes the mirror surface of the moving mirror not tilt during the reciprocating motion, so it can produce the light and dark change of the laser fringes, guaranteeing the subsequent equal optical path difference sampling. The linear motor can provide high-frequency and high-precision linear displacement and linear driving force for a precision position servo system[14], so it is selected as the driving source. The moving mirror is doing reciprocating linear motion driven by the linear motor. Therefore, the control of the moving mirror can be transformed into the control of the linear motor. Compared with Pulse Width Modulation (PWM), the control accuracy of a Digital Analog Converter (DAC) plus linear power amplifier is much higher, and there will be no high-order harmonic interference of PWM. Therefore, in this paper's moving mirror system, we use DAC and linear power amplifier as the motion actuator. The total control voltage U_{add} equals the feedforward control voltage $U0$ plus the speed feedback control voltage ΔU.

2 Design of the control algorithm

2.1 Design of the speed measuring algorithm

There is a reference laser interference system in the moving mirror system of the FTS. When the moving mirror moves, a beam of reference laser is reflected and modulated by the moving mirror. The other beam of reference laser is reflected by the fixed mirror. The two reflected reference lasers are combined by a beam splitter to form the laser interference signal. The optical path difference of the laser interference signal is twice the moving mirror's displacement, that is, the moving mirror moves $\lambda/2$ generating a laser interference signal, where λ is the laser wavelength.

The motion cycle of the moving mirror is Tms. Assuming that the control cycle is $t_0$ms, the whole travel of the moving mirror is divided into N segments, $N=T/t_0$. It is designed to measure speed in the first $\frac{t_0}{2}$ of each t_0 and generate the feedback control voltage in the second $\frac{t_0}{2}$. In this paper, we adopt the T-method to measure speed. The speed is calculated by the real time that the moving mirror takes to move a known distance. The specific principle is shown in Figure 2. As shown in Equation (1), $laser(i)$ is the number of expected laser interference signals in $[2(i\text{-}1)\frac{t_0}{2}, (2i\text{-}1)\frac{t_0}{2}]$ $(1\leqslant i\leqslant N)$, $realt(i)$ is the clocks of the real time taken to generate $laser(i)$ signals, $v(i)$ is the average speed. $realt(i)$ can be measured with a high-frequency local clock, and fs is the local clock frequency. In this system, fs is 5MHz. Since there is a one-to-one inversely proportional relationship between $realt(i)$ and $v(i)$, when $laser(i)$ is fixed, $realt(i)$ can be used to represent the real speed of the moving mirror in the current control cycle. When the expected motion law of the moving mirror is unchanged, $\frac{laser(i)\cdot\frac{\lambda}{2}}{v(i)}$ is a constant value in the i_{th} control cycle, and the measurement accuracy is proportional to fs. The larger the fs, the higher the measurement accuracy; the smaller the fs, the lower the measurement accuracy. When t_0 is 1 ms, the measurement accuracy is 0. 04%.

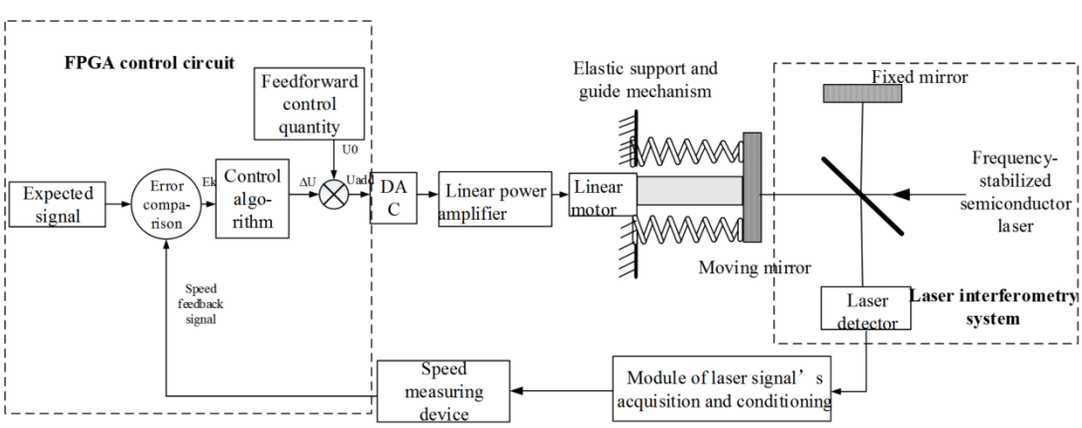

Fig. 1 The moving mirror speed control system
图1 动镜速度控制系统框图

$$realt(i)=\frac{laser(i)\cdot\frac{\lambda}{2}}{v(i)}\cdot fs, \tag{1}$$

2.2 Design of set values in speed-loop controller

Because the T-method is used to measure speed in this paper, the expected speed can also be represented by the clocks of $laser(i)$. We define the clocks as $expect(i)$. Ideally, the time of $laser(i)$ is $\frac{t_0}{2}$ms. But in the actual system, in $j*\frac{t_0}{2}(0\leqslant j\leqslant 2N)$, the $laser(i)$ is not necessarily an integer. So we need to calculate the time approximating to $\frac{t_0}{2}$ms in which the $laser(i)$ is an integer. According to the following equations, we can deduce the $laser(i)$. Then the control cycle $t_0(i)$ and the expected speed $expect(i)$ can be deduced according to the inversely proportional relationship between time and displacement.

Firstly, the motion equations of the moving mirror velocity $v(t)$ and displacement $x(t)$ are established. In a one-way motion, the relationship between velocity $v(t)$ and time t is shown in Equation (2).

$$v(t)=\begin{cases} v_m\cdot\sin\left(\frac{\pi}{2}\cdot\frac{t}{t_1}\right) & 0\leqslant t<t_1 \\ v_m & t_1\leqslant t<T-t_1 \\ v_m\cdot\sin\left(\frac{\pi}{2}\cdot\frac{T-t}{t_1}\right) & T-t_1\leqslant t\leqslant T \end{cases}, \tag{2}$$

Where v_m is the velocity in the uniform region, T is the motion period and t_1 is the time of the accelerating section. The relation between displacement $x(t)$ and time t can be obtained by integrating Equation (2), as shown in Equation (3).

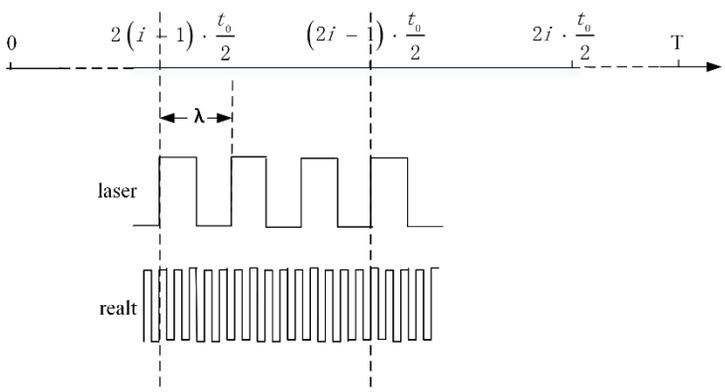

Fig. 2 The schematic diagram of T-method Measuring Speed
图2 T法测速示意图

$$x(t)=\begin{cases} \frac{-2t_1}{\pi}\cdot v_m\cdot\left[\cos\left(\frac{\pi}{2}\cdot\frac{t}{t_1}\right)-1\right] & 0\leqslant t<t_1 \\ v_m\cdot(t-t_1)+\frac{2t_1}{\pi}\cdot v_m & t_1\leqslant t<T-t_1 \\ v_m\cdot(T-2t_1)+\frac{2t_1}{\pi}\cdot v_m+\frac{2t_1}{\pi}\cdot v_m\cdot\cos\left(\frac{\pi}{2}\cdot\frac{T-t}{t_1}\right) & T-t_1\leqslant t\leqslant T \end{cases}, \tag{3}$$

$$b(t)=\begin{cases} \frac{-4t_1}{\lambda\pi}\cdot v_m\cdot\left[\cos\left(\frac{\pi}{2}\cdot\frac{t}{t_1}\right)-1\right] & 0\leqslant t<t_1 \\ \frac{2v_m}{\lambda}\cdot(t-t_1)+\frac{4t_1}{\lambda\pi}\cdot v_m & t_1\leqslant t<T-t_1 \\ \frac{2v_m}{\lambda}\cdot(T-2t_1)+\frac{4t_1}{\lambda\pi}\cdot v_m+\frac{4t_1}{\lambda\pi}\cdot v_m\cdot\cos\left(\frac{\pi}{2}\cdot\frac{T-t}{t_1}\right) & T-t_1\leqslant t\leqslant T \end{cases}, \tag{4}$$

Since the moving mirror moves $\lambda/2$ generating one laser interference signal, dividing $x(t)$ by $\lambda/2$ can obtain the number of laser interference signals $b(t)$ corresponding to the moving mirror displacement, as shown in Equation (4). Substitute $t=j*\frac{t_0}{2}$ into Equation (4) and round the result to the nearest integer, denoted as $b(j)$. By subtracting the even term $b(2(i-1))$ from the adjacent odd term $b(2i-1)$, we can obtain the $laser(i)$.

$$laser(i)=b(2i-1)-b(2(i-1))\quad 1\leqslant i\leqslant N, \tag{5}$$

Find the inverse function of Equation (4) to obtain Equation (6).

$$t(b)=\begin{cases}\dfrac{2t_1}{\pi}\cdot\cos^{-1}\left[\left(\dfrac{\lambda}{2}\cdot b-\dfrac{2t_1\cdot v_m}{\pi}\right)\cdot\left(\dfrac{-\pi}{2t_1\cdot v_m}\right)\right] & 0\leqslant b<\dfrac{4t_1v_m}{\pi\lambda}\\ \dfrac{\lambda\cdot b}{2v_m}-\dfrac{2t_1}{\pi}+t_1 & \dfrac{4t_1v_m}{\pi\lambda}\leqslant b<\dfrac{2v_m\left[2t_1+\pi\left(T-2t_1\right)\right]}{\pi\lambda}\\ T-\dfrac{2t_1}{\pi}\cos^{-1}\left[\dfrac{\pi}{2t_1}\left(\dfrac{\lambda\cdot b}{2v_m}-\dfrac{2t_1}{\pi}-T+2t_1\right)\right] & \dfrac{2v_m\left[2t_1+\pi\left(T-2t_1\right)\right]}{\pi\lambda}\leqslant b\leqslant\dfrac{2v_m\left[4t_1+\pi\left(T-2t_1\right)\right]}{\pi\lambda}\end{cases},\tag{6}$$

Then $t(b(j))$ is the time we mentioned earlier that we need to obtain. The analysis reveals that the difference between adjacent even terms of $t(b(j))$ is the theoretical control cycle, multiplied by the local clock frequency *fs* to obtain the clocks $t_0(i)$ corresponding to the control cycle. Furthermore, by multiplying the difference between adjacent odd and even terms by *fs*, we can obtain the clocks $expect(i)$ corresponding to the expected speed.

$$t_0(i)=\left[t\left(b(2i)\right)-t\left(b\left(2(i-1)\right)\right)\right]\cdot fs\quad 1\leqslant i\leqslant N,\tag{7}$$

$$expect(i)=\left[t\left(b(2i-1)\right)-t\left(b\left(2(i-1)\right)\right)\right]\cdot fs\quad 1\leqslant i\leqslant N,\tag{8}$$

In the actual system, the $laser(i)$, $t_0(i)$, and $expect(i)$ constitute the expected set values of the speed controller discussed in this paper.

2.3 Design of the feedforward control algorithm

The moving mirror motor of the control system in this paper is a linear motor, and its mathematical model is shown in Figure 3. We can deduce the feedforward control voltage *U0* from the voltage and current relationship of each circuit. In the model, *L* is the coil inductance, *R* is the coil resistance, K_f is the motor force constant, K_x is the axial stiffness of the spring, K_{be} is the back electromotive force (EMF) coefficient, *m* is the mover mass, *β* is the voltage gain of the power amplifier and *S* is the factor of the Laplace transform.

In Circuit I and Circuit II, there are Equations (9) and (10) respectively.

$$L\cdot\frac{dI(t)}{dt}+R\cdot I(t)=\beta\cdot U0(t)-K_{be}\cdot v(t),\tag{9}$$

$$K_f\cdot I(t)-K_x\cdot x(t)=m\cdot a(t),\tag{10}$$

In the motor, the value of $L\cdot\dfrac{dI(t)}{dt}$ is very small compared with $R\cdot I(t)$, so the inductance *L* is ignored in the equation. The calculation formula of $U0(t)$ is obtained by combining the two equations.

$$U0(t)=\frac{1}{\beta}\left[\left(m\cdot a(t)+K_x\cdot x(t)\right)\frac{R}{K_f}+K_{be}\cdot v(t)\right],\tag{11}$$

Where $v(t)$ is the Equation (2) in Section 2.2; $a(t)$ is the function of acceleration *a* and time *t*, which can be obtained by deriving $v(t)$ from *t*, $a(t)=\dfrac{dv(t)}{dt}$; $x(t)$ is the function of displacement *x* and time t, which can be obtained by integrating $v(t)$ with t, $x(t)=\int v(t)dt$.

Since the moving mirror control system is a digital controller, it is necessary to obtain the feedforward voltage of each time $i*t_0$. According to Section 2.2, the time when the number of laser interference signals is an integer and the closest to $i*t_0$ is $t(b(2i))$, substituting into Equation (11), $U0(t(b(2i)))$ is the speed feedforward voltage. The measured motor parameters are shown in Table 1. By substituting them into the formula, the specific voltage can be calculated. Although the motor parameters are obtained through experimental measurements, there will still be measurement errors. Under open-loop control with only feedforward voltage, the desired speed cannot be achieved. Additionally, if the moving mirror is affected by external mechanical disturbances, the speed uniformity will further deteriorate. Therefore, it is necessary to combine speed feedback control to eliminate the effects of parameter deviations and mechanical disturbances, improving the control system performance.

2.4 Design of the speed controller

The speed control system uses the most classical PID control as the system correction controller. In the second $\dfrac{t_0}{2}$ of the i_{th} control cycle, the speed error $Ek(i)$ is obtained by subtracting the $realt(i)$ and the $expect(i)$,

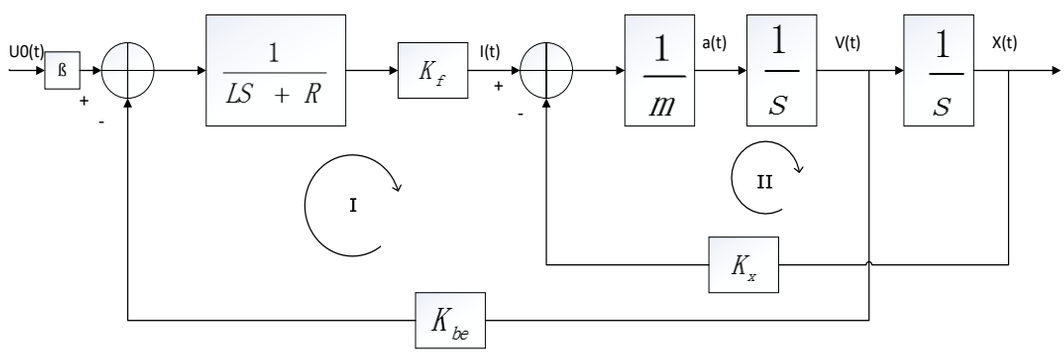

Fig. 3 The mathematical mode of the Motor
图3 电机数学模型

Table 1 Motor parameters.
表1 电机参数.

Parameter	Value
m	454g
R	3Ω
L	0.99mH
K_f	5.43N/Amp
K_{be}	5.43V/(m/s)
K_x	368N/m

that is, $Ek(i)=expect(i)-realt(i)$. Then the PID calculation of the error $Ek(i)$ is carried out to obtain the current PID control quantity $\Delta U(i)$.

$$\Delta U(i) = K_P \cdot Ek(i) + T_I \sum_{j=0}^{i} Ek(j) + T_D\left[Ek(i) - Ek(i-1)\right], \quad (12)$$

Where K_p, T_I, and T_D are proportional, integral, and differential parameters, respectively; $Ek(i-1)$ is the speed error of the $i-1_{\text{th}}$ control cycle.

Then the previous cycle's PID control quantity $\Delta U(i-1)$ is expressed as Equation (13).

$$\Delta U(i-1) = K_P \cdot Ek(i-1) + T_I \sum_{j=0}^{i-1} Ek(j) + T_D\left[Ek(i-1) - Ek(i-2)\right], \quad (13)$$

Subtract two equations to obtain the expression of the incremental PID control algorithm, as shown in Equation (14).

$$\Delta U(i) = \Delta U(i-1) + \left(K_P + T_I + T_D\right)Ek(i) + \left(-K_P - 2T_D\right)Ek(i-1) + T_D \cdot Ek(i-2), \quad (14)$$

Where the initial values of $\Delta U(i)$, $Ek(i)$, $Ek(i-1)$, $Ek(i-2)$ are 0.

The total control voltage $Uadd(i)$ of the i_{th} control cycle is equal to the feedforward voltage $U0(i)$ plus the PID control voltage $\Delta U(i-1)$ calculated in the $i-1_{\text{th}}$ control cycle.

$$Uadd(i) = U0(i) + \Delta U(i-1), \quad (15)$$

The PID parameters in this paper are tuned using the traditional Ziegler-Nichols method. In the experimental section, the same set of parameters is used both with and without vibration.

3 Results

In this paper, the A3PE3000 FG484 chip is selected as the control chip. It boasts 3 million logic gates and supports system performance up to 350MHz. The main clock frequency chosen for this study is 20MHz, and a 5MHz speed measurement clock is derived through internal frequency division within the FPGA. The control algorithm's software program is written and implemented in the Libero v9.1 development environment. Based on the FTS experimental platform, the performance verification experiment of the T-method composite speed controller is carried out. The block diagram of the experimental system and the experimental platform are shown in Figures 4 and 5. The computer is utilized for issuing commands and data acquisition, while the self-developed interferometer controller outputs control voltages to the interferometer. The control voltage, generated by the Data Physics DP 700 controller, is amplified by the Power Amplifier type BAA 120, and then transmitted to the TIRA GmbH S 51110-M actuator. Ultimately, the actuator outputs vibration excitation to the interferometer. An acceleration sensor is attached to the base plate of the interferometer, providing real-time acceleration feedback in the moving mirror motion direction to the actuator's controller for internal feedback control.

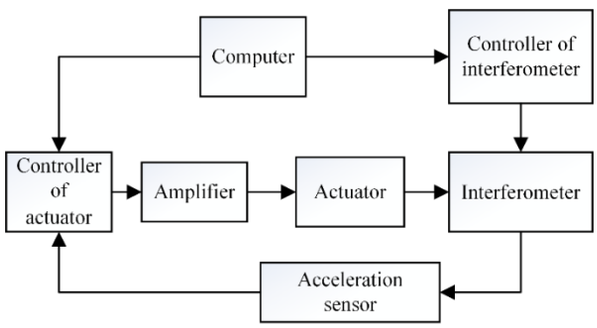

Fig. 4 The block diagram of the experimental system
图4 实验系统框图

The high-speed data acquisition card to collect the laser interference signal with a 2M clock, as shown in Figure 6.

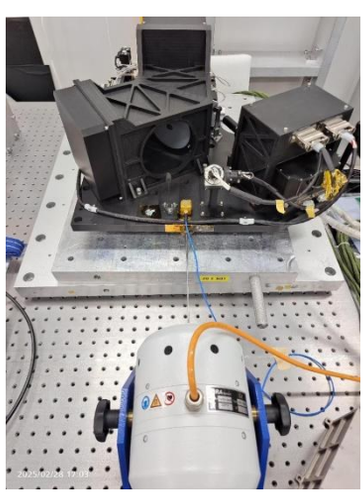

Fig. 5 The experimental platform
图5 实验平台

Count the number of sampling points n_k in the k_{th} laser interference signal, then the frequency of the laser interference signal is $f = \frac{2 \times 10^6}{n_k}$. Furthermore, the period of the laser interference signal is $T = \frac{1}{f} = \frac{n_k}{2 \times 10^6}$. According to the principle of Michelson interference splitting, a complete laser interference signal is generated when the moving mirror moves $\frac{\lambda}{2}$, so the moving mirror speed corresponding to the k_{th} laser interference signal is $V_k = \frac{\lambda/2}{T} = \frac{2 \times 10^6 \lambda}{2n_k}$, where λ is the laser wavelength. Using this method, the moving mirror speed of each laser interference signal is obtained in turn, and all the speeds are drawn into the velocity curve of the moving mirror. Then according to Equations (16) and (17), the peak-to-peak velocity error V_{PP} and the RMS velocity error V_{RMS} of the moving mirror can be calculated.

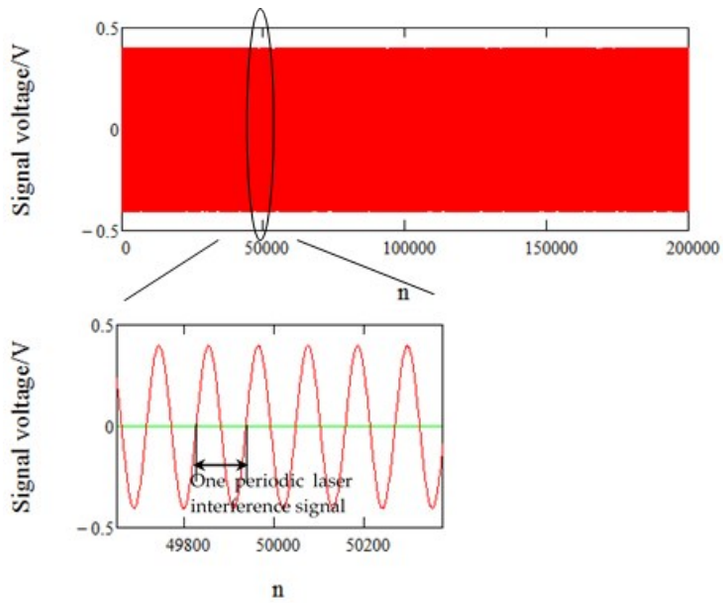

Fig. 6 Laser interference signal sampled with a 2 MHz clock and its partially enlarged image
图6 2M时钟采样的激光干涉信号和它的局部放大图

$$V_{PP} = \frac{V_{MAX} - V_{MIN}}{V_A}, \tag{16}$$

$$V_{RMS} = \frac{\sqrt{\frac{\sum_0^q (V_k - V_A)^2}{q}}}{V_A}, \tag{17}$$

where V_A is the average velocity; q is the number of laser interference signals contained in the uniform region; V_{MAX} and V_{MIN} are the maximum and minimum of the velocity.

When the control period is t_0 ms, the moving mirror of the FTS is controlled to move back and forth by the control system based on the T-method combined with speed feedforward, and the velocity curve without vibration is obtained as shown in Fig. 7.

To eliminate the possibility of randomness in the experimental data, we collected ten sets of velocity curves and calculated each V_{PP} and V_{RMS}, as shown in Table 2. Therefore, under the control system proposed in this paper, the V_{PP} of the moving mirror is 0.0182, and the V_{RMS} is 0.0027. In the literature[8], the final control effect is that the V_{PP} in the uniform region is 0.088, and the V_{RMS} is 0.014.

The moving mirror is a precision component, which is easily disturbed during the movement, and its working environment difficultly ensures that it is always on a static platform with a vibration level of less than 0.1 mg[15]. Therefore, we designed a micro-vibration experiment to test the anti-interference ability of the moving mirror in the composite speed control system using the T-method. Fix the FTS on the single-degree-of-freedom micro-excitation platform and apply 5mg, 7.5 mg, and 10 mg sine excitation in the moving mirror motion direction to simulate external interference respectively. Conduct constant frequency excitation at integer frequency points ranging from 2 to 200 Hz (with an interval of 2 Hz from 2 to 120 Hz and 5 Hz from 120 to 200 Hz). Test the speed uniformity of the moving mirror, and record the V_{PP} and V_{RMS} at each frequency point. The results are shown in Figures 8 and 9. The maximum velocity error is at 50 Hz. Under the 5 mg, 7.5 mg, and 10 mg vibration, the max V_{PP} is 0.0724, 0.1087, and 0.1405 respectively, and the max V_{RMS} is 0.0225, 0.0334, and 0.0448. The velocity error is basically proportional to the excitation magnitude, as shown in Fig. 10.

The max V_{PP} of 5 mg, 7.5 mg, and 10 mg are used as the FTS spectral inversion input respectively. A simulation analysis assesses the impact of only the moving mirror's speed errors on spectrum stability. The resulting laser spectrum histograms for each speed error are shown in Fig. 11, where the vertical axis represents the frame index of the samples, and the horizontal axis represents the peak wavenumber of each inverted laser spectrum.

The spectrum stability can be calculated by Equation (18), where *SS* is the spectrum stability and *Peak* is the peak wavenumber. From the simulation results, it is evident that the spectrum stability of the FTS increases with the speed error. When the speed error is 0.1405, the spectrum stability is 0.14 ppm.

Table 2 Ten sets of V_{PP} and V_{RMS}.
表2 10组VPP和VRMS.

	1	2	3	4	5	6	7	8	9	10
V_{PP}	0.01819	0.01819	0.01819	0.01819	0.01819	0.01819	0.01819	0.01819	0.01819	0.01819
V_{RMS}	0.00271	0.00268	0.00274	0.00267	0.00273	0.00267	0.00271	0.00266	0.00271	0.00270

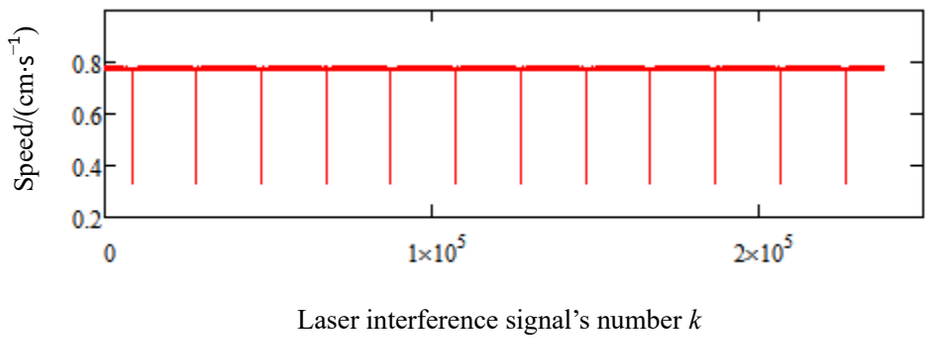

（a）

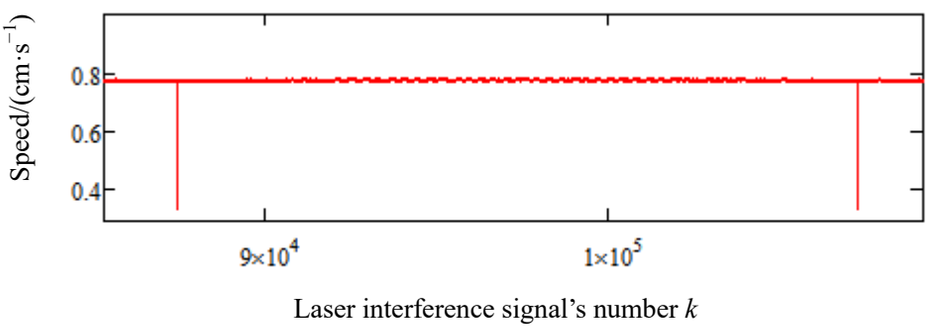

（b）

Fig. 7 Velocity curves of the moving mirror(the absolute value of speed in uniform region): (a) Multiple sets of velocity curves; (b) A one-way velocity curve
图7 动镜速度曲线(匀速区速度绝对值):(a) 多组速度曲线;(b)单程速度曲线

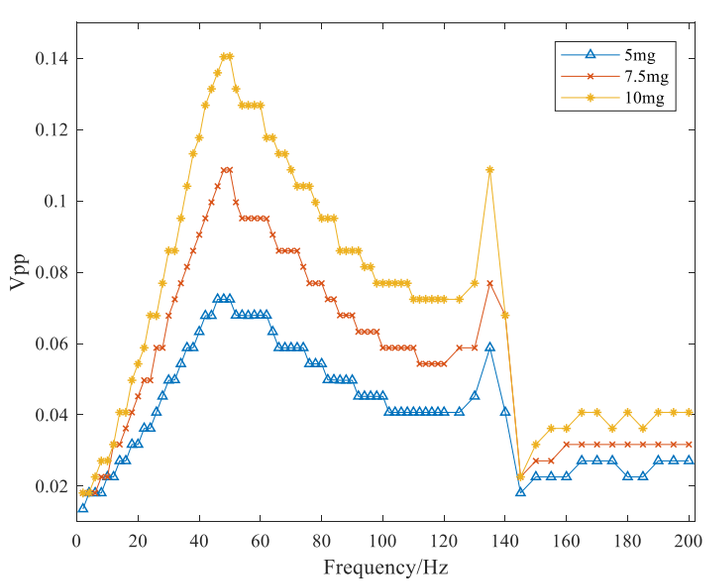

Fig. 8 The V_{PP} of the moving mirror under 5 mg, 7. 5 mg, and 10 mg sine excitation over 2-200 Hz
图8 5 mg,7. 5 mg,10 mg正弦激励下,2~200 Hz范围内动镜速度峰峰值误差

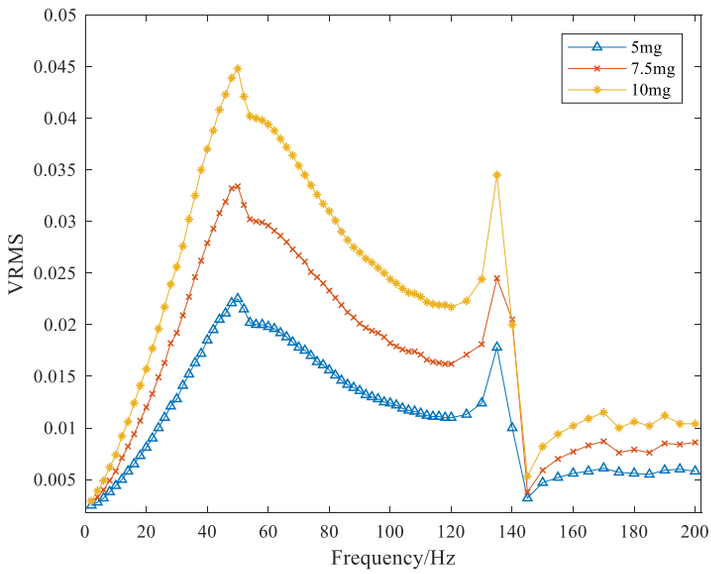

Fig. 9 The V_{RMS} of the moving mirror under 5mg, 7. 5mg, and 10mg sine excitation over 2-200Hz
图9 5 mg,7. 5 mg,10 mg正弦激励下,2~200 Hz范围内动镜速度均方根值误差

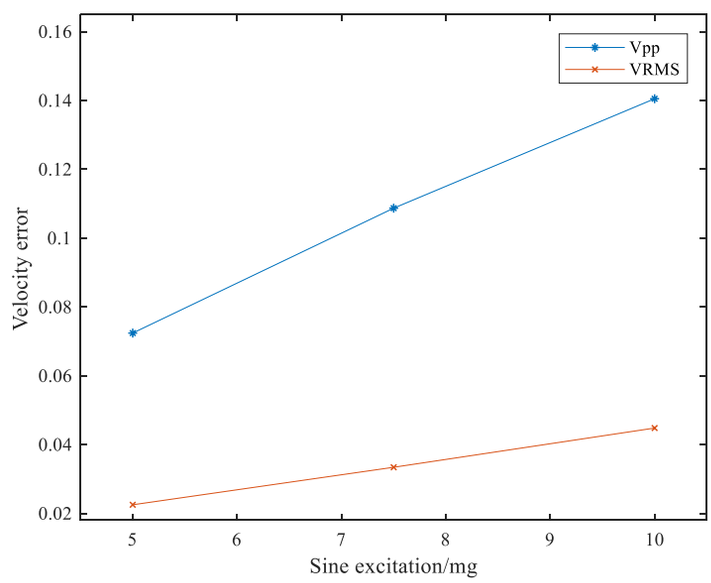

Fig. 10 The relationship between velocity error and sine excitation
图10 速度误差和振动量级的关系图

$$SS = \frac{\max(Peak) - \min(Peak)}{mean(Peak)}, \tag{18}$$

The performance metric for this FTS is a spectrum stability of less than 2ppm, which means that the moving mirror velocity uniformity of 10mg still meets the spectrum stability requirement. The spectral resolution after inversion is 0. 625 cm^{-1}, as shown in Fig. 12, which also satisfies the performance requirements of the FTS.

Additionally, the integrating infrared focal plane detector integrates the interference signal at each equal optical path difference sampling interval, thus requiring the timing error of the sampling interval, which is generally less than 15%. Since the optical path difference for each sampling interval is fixed and equal to the reference laser wavelength λ, the V_{PP} of the moving mirror at each sampling interval must also be less than 15%. The experimental results indicate that under a 10mg sine excitation, the V_{PP} of the moving mirror in this system is 14. 05%, which also meets the application requirement of the integrating infrared focal plane detector.

4 Conclusions

Through literature research, we know that the exist-

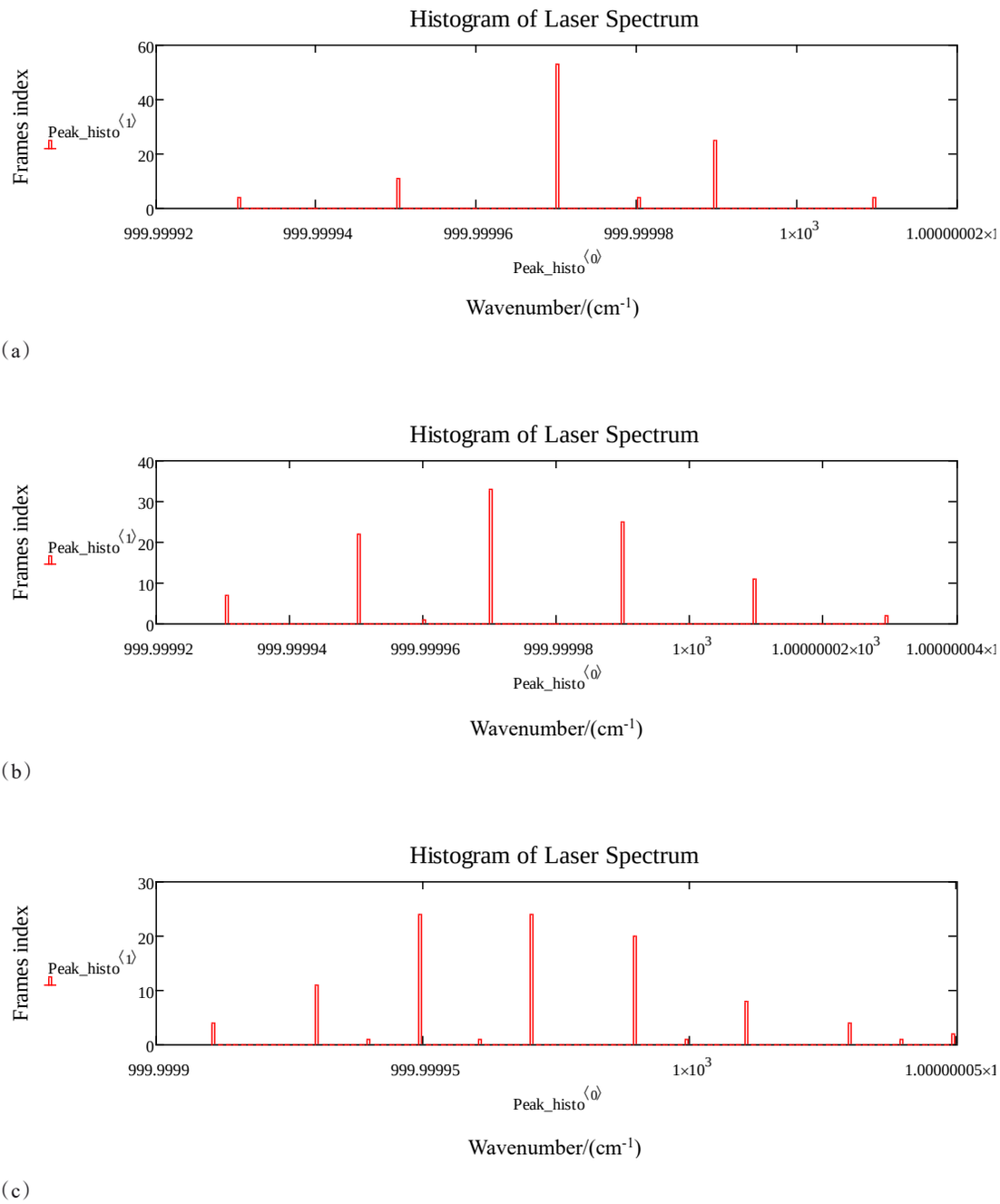

Fig. 11 Laser spectrum Histograms at different speed errors: (a) Speed error is 0.0724; (b) Speed error is 0.1087; (c) Speed error is 0.1405

图 11 不同速度误差下的激光光谱直方图:(a) 速度误差是 0.0724;(b) 速度误差是 0.1087;(c) 速度误差是 0.1405

ing moving mirror speed control schemes of the FTS include single position-loop control based on M-method, position-loop control based on M-method combined with feedforward control, and single speed-loop control based on T-method. In this paper, we design and implement a new moving mirror speed control system based on T-method combined with speed feedforward, and achieve good control effect. Under the condition of no vibration, using the new control system, the V_{PP} in the uniform region is 0.0182, and the V_{RMS} is 0.0027; Under the unidirectional sine excitation with the amplitude of 10mg and the frequency of 2-200Hz, using the new control system, the max V_{PP} is 0.1405, and the max V_{RMS} is 0.0448. Analyzing both the spectrum stability and the integration time of the infrared focal plane detector, the velocity uniformity meets the performance requirements of the FTS.

Theoretically, the T-method can still have high measurement accuracy when the moving mirror moves slowly; After the feedforward control is introduced, the deviation regulated by the feedback control is reduced, there-

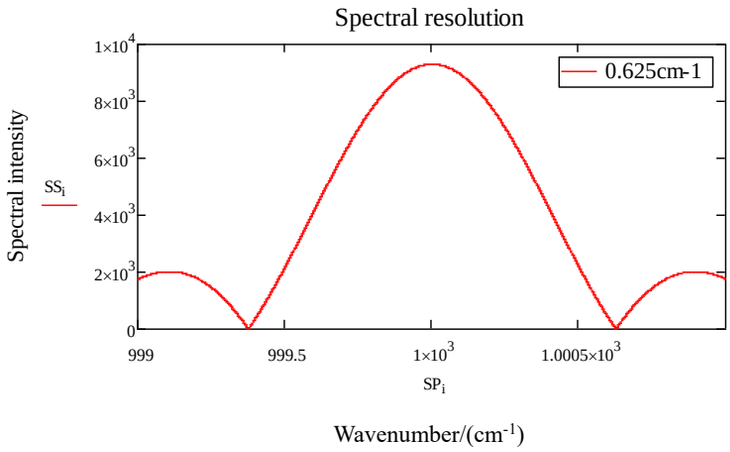

Fig. 12 Spectral resolution
图12 光谱分辨率图

by enhancing the response speed of the feedback loop, which increases the control bandwidth. This design provides a technical means for realizing the speed control of the moving mirror with low speed and high stability. Also, it makes the FTS have wider applications.

References

[1] HUA Jian-Wen, WANG Zhan-Hu, DUAN Juan, et al. Review of Geostationary Interferometric Infrared Sounder [J]. Chin. Opt. Lett, 2018, 16: 111203.
[2] Ronald J G, David C J, Peter M. Development of the Crosstrack Infrared Sounder (CrIS) Sensor Design [J]. SPIE, 2002, 4486: 441 - 469.
[3] Suto H, Kataoka F, Kikuchi N. Thermal and Near-infrared Sensor for Carbon Observation Fourier Transform Spectrometer-2 (TANSO-FTS-2) on the Greenhouse Gases Observing SATellite-2 (GOSAT-2) during Its First Year in Orbit[J]. Atmos. Meas. Tech, 2021, 14: 2013 - 2039.
[4] LI Qi, DU Biao, ZHANG Zheng-Dong, et al. Application of Fourier Transform Near-Infrared Spectrometer in Gasoline and Diesel Analysis[J]. Metrology Science and Technology, 2022, 66(10): 20-27.
(李琪,杜彪,张正东,等.傅里叶变换近红外光谱仪在汽、柴油分析中的应用[J].计量科学与技术),2022,66(10):20-27.
[5] SONG Xu-Yao, DONG Wei, PAN Yi-Jie, et al. The infrared spectral emissivity measurement of a graphite material in a high temperature range of 1000~1500℃ using integrated blackbody principle [J]. J. Infrared Millim.Waves, 2021, 40(02): 204-213.
(宋旭尧,董伟,潘奕捷,等.基于集成黑体法1000～1500℃石墨材料高温红外光谱发射率测量[J].红外与毫米波学报),2021,40(02):204-213.
[6] BAO Wei. Measurement of sea surface emissivity at large viewing angle using Fourier spectrometer[J]. Science and Technology & Innovation, 2024, (09): 95-97.
(包维.利用傅里叶光谱仪进行大观测角度下海表发射率测量[J].科技与创新),2024,(09):95-97.
[7] XIA Xiang. Research on Technology of Multi-Speed Mode Canning of Interference Spectrometer [D]. Shanghai: Shanghai Institute of Technical Physics, 2014.
(夏翔.干涉光谱仪多速度模式扫描技术研究[D].中国科学院研究生院(上海技术物理研究所)),2014.
[8] DUAN Juan, HUA Jian-Wen, WANG Hai-Ying. Digital Control of Moving Mirror Motor in Fourier Transform Spectrometer Based on FPGA[J]. Micromotors, 2015, 48(09): 62 - 65.
(段娟,华建文,王海英.基于FPGA的星载傅里叶光谱仪动镜电机的数字控制[J].微电机),2015,48(09):62-65.
[9] Marc-Andre A.S, Francios C, Christophe D,et al. ACE-FTS Instrument Detailed Design[J]. SPIE, 2002, 4814: 70-81.
[10] Bruce C L, James W J, Steven H S, et al. Miniaturization of the thermal emission spectrometer (TES) electronics for the Mars 2001 Lander[J]. SPIE, 1999, 3756: 555-563.
[11] SUN Fang, DAI Zuo-Xiao, HUA Jian-Wen, et al. A Speed Measuring System of Moving Mirror for Fourier Transform Spectrometer[J]. Semiconductor Optoelectronics, 2007, (02): 283-286.
(孙方,代作晓,华建文,等.一种傅里叶变换光谱仪动镜速度测量系统[J].半导体光电),2007,(02):283-286.
[12] Denis S, Patrick A, Didier M, et al. Design and development of IASI instrument[J]. SPIE, 2004, 5543: 208-219.
[13] Darryl E Weidler. Mechanical design of GHIS brassboard[J]. SPIE, 1996, 2812: 479-488.
[14] QIU Jin-Shan. Study on Drive Control of Linear Electromagnetic Actuator[D]. Chongqing University, 2016.
(邱金山.直线电磁作动器的驱动控制研究[D].重庆大学,2016.
[15] DONG Yao-Hai, ZHOU Xu-Bin, SHEN Jun-Feng, et al. Study on Micro-Vibration Suppression Technology of FY-4 Satellite[J]. Aerospace Shanghai, 2017, 34(04): 20-27.
(董瑶海,周徐斌,申军烽,等.FY-4卫星微振动抑制技术研究[J].上海航天),2017,34(04):20-27.